JOURNAL OF APPLIED ELECTROCHEMISTRY 20 (1990) 677–685

Electrochemical impedance spectroscopy on porous electrodes

L. M. GASSA, J. R. VILCHE

Instituto de Investigaciones Fisicoquimicas Teoricas y Aplicadas (INIFTA), Universidad Nacional de La Plata, Sucursal 4, C. C. 16, 1900 La Plata, Argentina

M. EBERT, K. JÜTTNER, W. J. LORENZ

Institut für Physikalische Chemie und Elektrochemie III, Universität Karlsruhe, Kaiserstrasse 12, D-7500 Karlsruhe 1, FRG

Received 10 July 1989; revised 22 September 1989

Electrochemical d.c. and a.c. measurements have been carried out on porous Raney nickel in H_2-saturated 0.1 M, 1 M, and 6 M NaOH solutions at $T = 303$ K and 333 K using rotating-disc and static-planar electrodes. For comparison, measurements were also performed on graphite-cloth and graphite-felt electrodes. From polarization curves and current transients obtained in the potential range of the hydrogen evolution and hydrogen oxidation reactions the dependence of the electrocatalytic activity of Raney nickel on the prepolarization conditions was studied. Impedance spectra in the frequency range $1\,\text{mHz} \leqslant f \leqslant 10\,\text{kHz}$ were used to determine the characteristic pore parameters and to identify the kinetic behaviour of the porous electrodes by application of transfer function analysis using non-linear fit routines.

1. Introduction

Porous structures are of practical importance in technical applications as catalyst material for different heterogeneous chemical and electrochemical processes [1–3]. The main characteristic parameters of the porous materials are the length, the diameter, and the number of pores, their geometric profile, the specific area, and the degree of uniformity of the porous structure. In the case of gas-phase reactions, BET and X-ray diffraction, provide a quantitative determination of these parameters. However, for porous materials in contact with an electrolyte solution, the *in situ* characterization of the catalyst with respect to its structural and morphological properties is more complicated. The corresponding information may be obtained by applying indirect methods. The number of theoretical investigations on the steady-state polarization behaviour of porous electrodes is relatively large compared with the treatments of the transient response of flooded electrodes [4–7].

One of the most promising modern and dynamic techniques which can be applied today is provided by electrochemical impedance spectroscopy (EIS). The latter has already been used in some specific practical systems as well as for modelling of porous systems. The corresponding experimental results were interpreted in terms of electrical equivalent circuits [8–10], single (cylindrical) pore models with or without taking into account axial gradients of potential and concentration [11–19], whereas other treatments consider the porous material as isotropic and macroscopically homogeneous [20]. Most of the models are based on a simplified treatment of the system with respect to concentration and activation polarization in order to obtain analytical solutions, whereas the complicated case of coupled axial gradients of potential and concentration was only recently dealt with on the basis of a semi-analytical treatment [21].

In spite of the numerous theoretical contributions, the number of experimental studies is rather scanty. It is interesting to note that most of the impedance measurements were carried out either under quasi-equilibrium or under low-polarization conditions. Transfer function analysis based on a physical model and using non-linear fit routines has so far not been carried out intensively. It is the aim of this paper to demonstrate that transfer function is a possible means for the characterization of porous catalyst materials by use of EIS.

2. Experimental details

Electrochemical d.c. and a.c. measurements were carried out on three different porous materials, Raney nickel, graphite-cloth, and graphite-felt electrodes in H_2-saturated 0.1 M, 1 M and 6 M NaOH solutions at $T = 303$ K and 333 K. Electrolyte solutions were prepared from analytical grade (Merck) reagents and four-fold distilled water. The commercial Raney nickel electrodes (Varta Batterie AG) with nickel net as the electrical contact were used without further pretreatment. The thickness of the catalyst granules ranged from 2 to 10 μm as determined by SEM. Fig. 1

0021-891X/90 $03.00 + .12

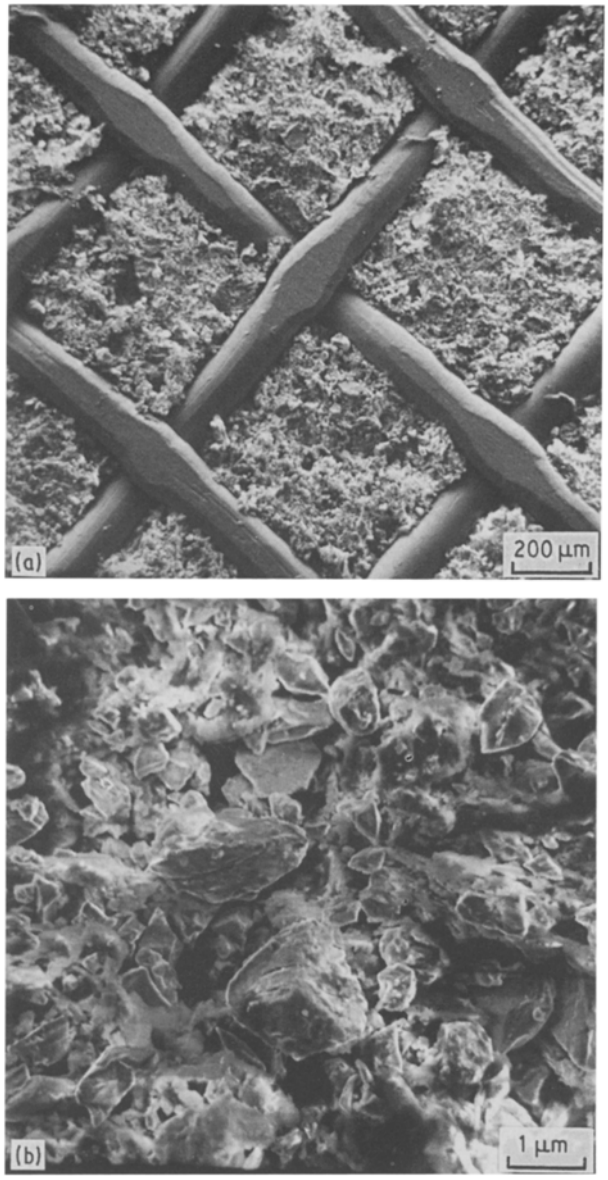

Fig. 1. SEM micrographs of Raney nickel at different magnifications: (a) the nickel grid for stabilization and for electrical contact and (b) the porous structure grain size of the material.

shows SEM micrographs of Raney nickel at different magnifications. The thickness of the electrode structure was about 1 mm. A detailed description of the technical production process is given elsewhere [22]. Rotating-disc electrodes of 0.28 cm^2 geometric area were prepared by fixing the porous catalyst on a rotating disc holder using epoxy resin with the nickel net on the solution side. These electrodes cannot be considered as ideal disc electrodes, nevertheless they do allow study of the influence of forced convection. Under static conditions, Raney nickel electrodes of 1 cm^2 geometric surface area and backed with a porous PTFE foil were used (Varta Batterie AG). Graphite-felt and graphite-cloth materials (GF-S3 and GC-10, The Electrosynthesis Corporation, Inc) of 0.5 mm thickness and 1 cm^2 geometric area were also employed under static conditions. For the sake of comparison some measurements were carried out using a high-purity, polycrystalline-nickel electrode. A conventional three compartment double-wall glass cell was kept at constant temperature using a thermostat (Lauda). For the measurements in 6 M NaOH solution, a PTFE cell was used. A large area platinum sheet was used as the counter electrode and a Hg/Hg_2O electrode in the same electrolyte served as the reference electrode with a Haber–Luggin capillary tip. Potentials (E_H) given in the text are referred to the NHE scale.

A Wenking potentiostat (LB 75L) with voltage sweep generator (VSG 72) and an X–Y recorder (HP 7004B) were used for the steady state and cyclic voltammetric measurements. Impedance spectra in the frequency range $1\,mHz \leqslant f \leqslant 10\,kHz$ were obtained using a Solartron frequency response analyser (FRA 1172) integrated with an HP 9845B computer system. For the impedance measurements and activated platinum probe was coupled to the reference electrode through a 6 μF capacitor to reduce phase errors at high frequencies.

3. Results and discussion

3.1. *d.c. measurements*

The d.c. behaviour of the Raney nickel electrodes was found to be strongly dependent on the NaOH concentration, on the temperature, and on the polarization routine. The open circuit potential of the electrode after immersion and prior to any polarization was not well defined, shifting between -0.6 V and -0.2 V. Typical quasi-steady-state current density potential curves obtained on a planar electrode under static conditions are shown in Fig. 2 for three different NaOH concentrations at constant temperature $T = 303$ K. At constant overpotentials, the overall activity of the electrode increases significantly with the concentration of NaOH. Similarly, an increase of the current densities by one order of magnitude was found when the temperature was raised to 333 K. Generally, a complete polarization cycle exhibits a typical hysteresis of the polarization curve. Starting the polarization from $E_H = 0$ V towards negative potentials, the cathodic current density increases only slightly and the hydrogen evolution at appreciable rate does not commence before $E_H \approx -0.8$ V is reached. Below this potential the cathodic current density increases steeply. At higher current densities the onset of a strong gas-evolution leads to a limitation of the hydrogen evolution reaction due to concentration and ohmic drop polarization. In 6 M NaOH the current density exceeds 1 $A\,cm^{-2}$ and therefore the polarization was restricted to lower overpotentials. In the reverse polarization direction the current density changes its sign around $E_H = -0.8$ V and attains a nearly potential-independent, positive limiting value. The corresponding anodic process is mainly associated with the oxidation of H_2 that is formed and stored in the pores of the electrode rather than with the oxidation of H_2 dissolved in the bulk solution. This can be concluded from the following facts:

(i) the reversal from cathodic to anodic current

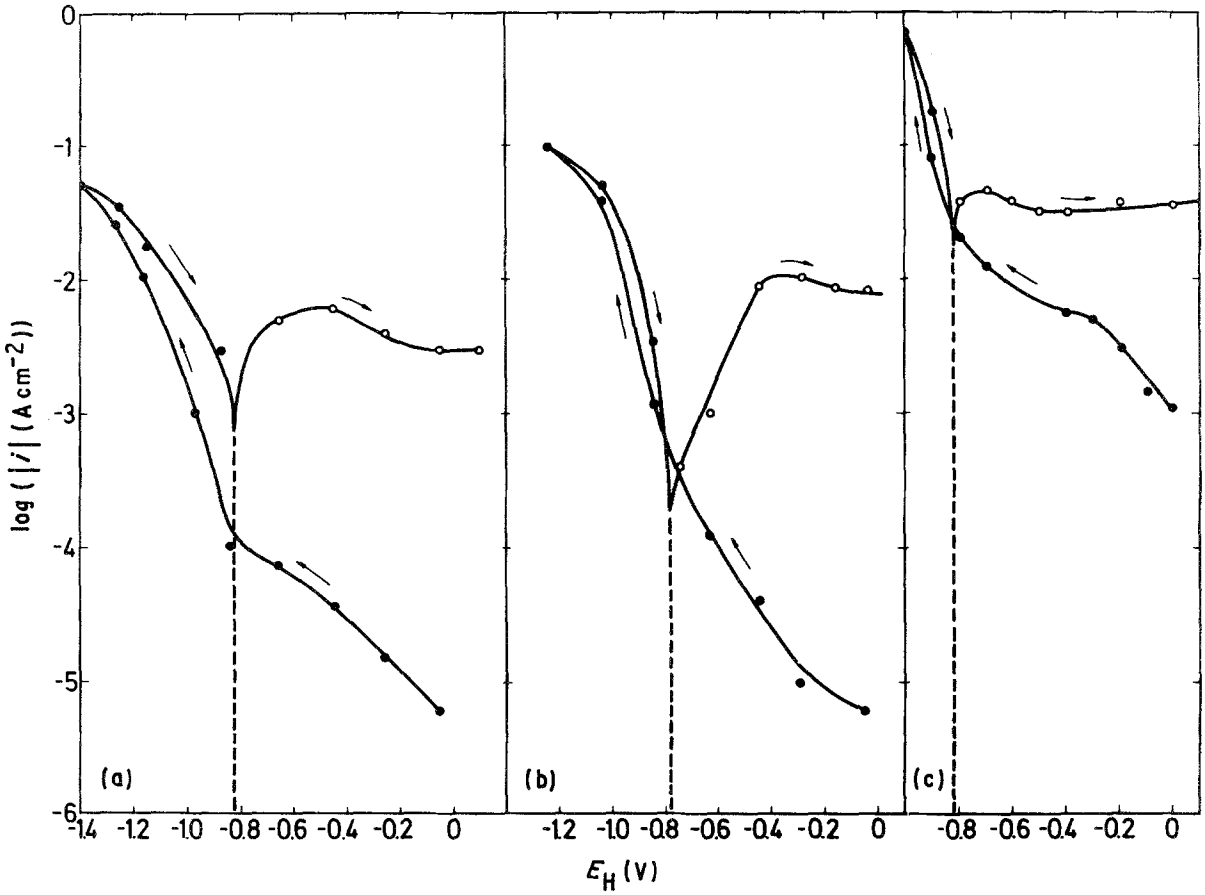

Fig. 2. Quasi-steady-state current density–potential curves of static, planar Raney nickel electrodes in (a) 0.1, (b) 1.0 and (c) 6 M NaOH solutions, H_2-saturated, $|dE/dt| = 10^{-3}\,V\,s^{-1}$.

takes place at the equilibrium potential of the H_2/H^+ electrode

(ii) the limiting anodic current density is independent of the electrode rotation speed or the stirring of the solution,

(iii) the anodic current slowly decays at constant potential

(iv) a positive current is not observed on a flat nickel sheet under the same conditions.

Studying the transient behaviour at a fixed potential, it was found that the anodic current decays slowly, following a linear i versus t^{-1} relationship. The time to reach a relatively low anodic current density of $i = 10^{-4}\,A\,cm^{-2}$ depends on the H_2 loading conditions in the potential range of the hydrogen evolution reaction. A decay time of typically 200 min was observed after loading the electrode at $E_H = -1.2\,V$ for 300 min. This time is sufficient to obtain impedance diagrams under quasi-stationary conditions in the anodic part of the polarization curves.

3.2. *a.c. measurements*

Fig. 3 shows a typical set of impedance diagrams obtained on a planar Raney nickel electrode under static conditions in 6 M NaOH. Starting the impedance measurements at potentials where the cathodic hydrogen evolution predominates, the impedance exhibits a strongly depressed capacitive semicircle at higher frequencies with the indication of a second time constant at lower frequencies. The depressed semicircle at high frequencies increases slightly with decreasing potential, whereas it disappears completely at potentials where the oxidation of H_2 predominates. In this potential range theabsolute values of the impedance and the location of the frequencies on the Nyquist plots are nearly independent of the applied d.c. potential. As a general characteristic feature, the high-frequency part of all impedance diagrams exhibits a slope close to unity corresponding to a phase angle of $-45°$. This behaviour is typical for porous systems, as will be discussed below.

The different states of the electrode, depending on the d.c. prepolarization (3.1), are also well reflected in the impedance behaviour. In Fig. 4 measurements at two different potentials in the cathodic and in the anodic range are compared before and after 30 min prepolarization at a high negative potential ($E_H = -1\,V$). The shape of the diagrams does not differ substantially but a higher activity of the electrode is indicated by the lower values of the overall impedance after the polarization. On the other hand, the transition from the unity-slope of the impedance in the high-frequency part to the second time constant at low frequencies is ill defined without prepolarization. Furthermore, an additional tail with almost zero slope is observed at high frequencies.

The influence of the NaOH concentration on the electrode activity is also evident from the impedance

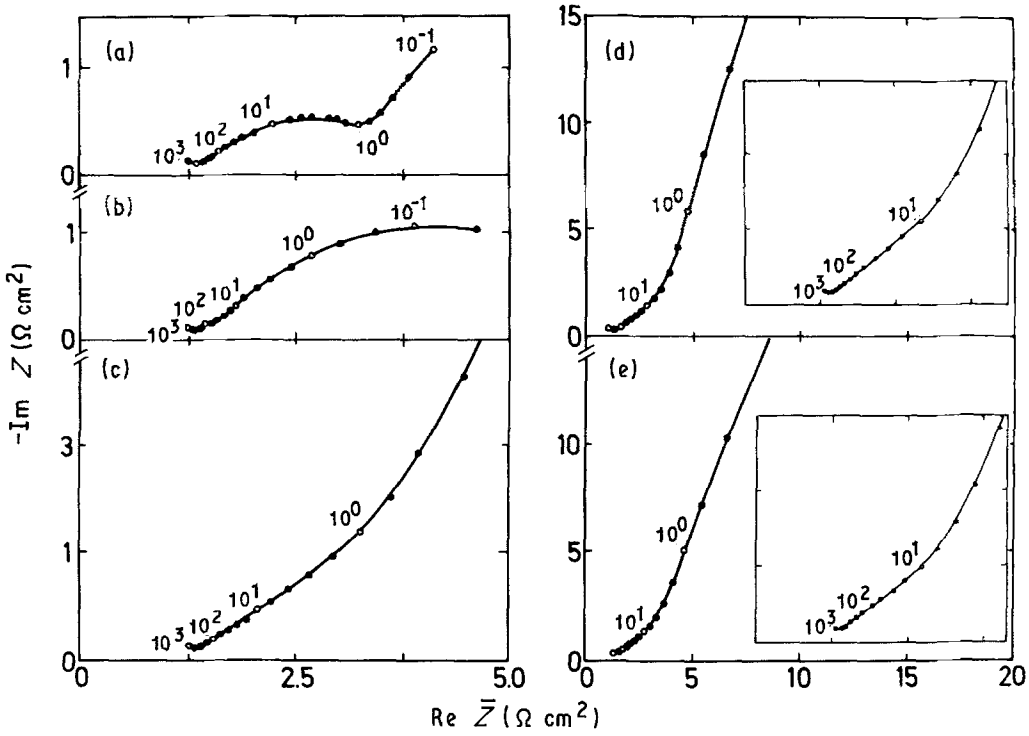

Fig. 3. Impedance diagrams in Nyquist representation obtained on static, planar Raney nickel electrodes in 6 M NaOH solution at $T = 303$ K and at electrode potentials, E_H, = (a) −0.9 V (b) −0.8 V (c) −0.7 V (d) −0.5 V and (e) −0.2 V. (d) and (e) contain a magnification of the high-frequency part.

diagrams shown in Fig. 5. In 0.1 M NaOH solution (Fig. 5a) the overall impedance differs by several orders of magnitude from those found in 1 M and 6 M NaOH solutions (Figs 5b and c), although the distribution of frequencies in the Nyquist diagrams remains nearly the same.

In order to study the effect of forced convection on the impedance behaviour, measurements were performed on a rotating-disc electrode in 1 M NaOH. Generally, it was found that electrodes of this type show a lower activity with respect to the steady-state current density and the magnitude of the impedance, whereas the shape of the Nyquist diagrams, Fig. 6, is similar to that of the planar electrodes under comparable polarization conditions, compare with Fig. 3a. The lower activity may be caused by the epoxy resin which partly penetrates into the pores of the electrode during its preparation. A similar dependence on the polarization conditions, as described above for planar electrodes, is found on the disc electrode, as can be seen from a complete set of impedance diagrams presented as Bode plots, $\log |Z|$ versus $\log f$, in Fig. 7. The impedance of the initially inactive electrode at $E_H = -0.2$ V is characterized by a purely non-ideal capacitive behaviour (Fig. 7a). With decreasing electrode potential, the polarization resistance, $R_p = \lim_{\omega \to 0} \{Z(j\omega)\}$, decreases and the impedance at $E_H = -1.4$ V resembles that of an RC parallel combination. On reversal of the polarization direction (Fig. 7b), the overall impedance increases again leading to a pure capacitive behaviour with absolute values of the impedance being one order of magnitude lower than those measured with decreasing potential (Fig. 7a).

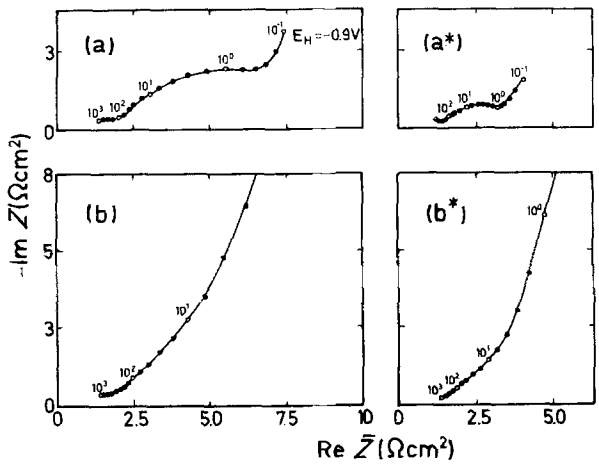

Fig. 4. Effect of prepolarization on the impedance measurements. Static, planar Raney nickel electrodes in 6 M NaOH solution at $T = 303$ K; Nyquist diagrams at potentials $E_H = -0.9$ V (a, a*) and $E_H = -0.3$ V (b, b*) where * indicates the measurements were made after about 30 min prepolarization at $E_H = -1.0$ V.

For comparison, impedance measurements were also performed on both graphite-cloth and graphite-felt electrodes to study the effect of different structure and porosity. These electrodes showed only low activity for the hydrogen evolution reaction, therefore they are of limited interest for technical applications. The impedance diagrams are mainly characterized by purely capacitive behaviour with the typical features of porous systems at high frequencies. Fig. 8 shows Nyquist diagrams obtained under comparable current density conditions on Raney nickel, graphite cloth (GC-10), and graphite felt (GC-S3). Both graphite electrodes were anodically activated at $E_H = 2$ V for $t = 2$ min. The impedance diagrams in Fig. 8 exhibit

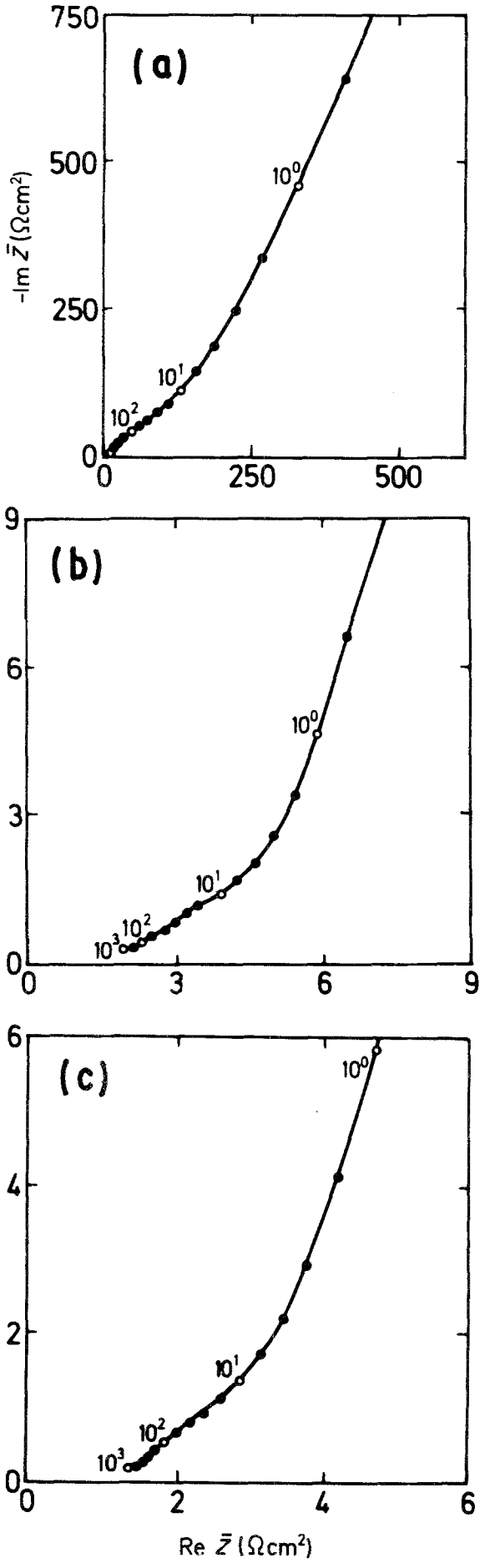

Fig. 5. Influence of NaOH concentration on the high-frequency part of the impedance diagrams of stationary, planar Raney nickel electrodes at $E_H = -0.3$ V; $T = 303$ K. (a) 0.1 (b) 1.0 and (c) 6 M NaOH.

a similar shape, however, differences in the magnitude and frequency disribution can be distinguished and will be discussed below.

3.3. *Model simulation*

The d.c. and a.c. measurements clearly show that the systems studied are highly complicated. A quantitative description of the results by a unique kinetic model is difficult because the structure of the system is too complex and some specific parameters are not available or not well known. However, the main features of the impedance measurements under different conditions can be explained at least semi-quantitatively using the cylindrical-pore model proposed by de Levie [11] and modified by other authors. The basic equation for the impedance of a single cylindrical pore is given by

$$Z_{pl}(s) = (1/\pi r)(\rho Z_0(s)/2r)^{1/2} \coth (2\rho l^2/rZ_0(s))^{1/2} \quad (1)$$

where r and l are the radius and the length of the pore, ρ is the specific resistivity of the electrolyte in the pores, and $Z_0(s)$ is the specific impedance per unit area of the flat electrode on the developed surface of a cylindrical pore with $s = j\omega$. For a pure charge-transfer-controlled process, neglecting transport effects, $Z_0(s)$ can be described by a parallel combination of a charge-transfer resistance, R_t, and the double-layer capacitance, C_{dl}. Taking into account heterogeneity effects of the catalyst material, the well-known dispersion formula

$$Z_0(s) = R_t/[1 + (sR_tC_{dl})^\alpha] \quad (2)$$

with an empirical exponent α ($0 < \alpha \leqslant 1$) will be used in the following. The overall impedance, Z_p, of a porous electrode, which consists of n identical pores in parallel, is then given by

$$Z_p(s) = R_{el} + Z_{pl}(s)/n \quad (3)$$

where R_{el} is the uncompensated electrolyte resistance between the reference electrode and the surface plane of the working electrode. This equation was found to fit sufficiently well most of the above-described impedance results on Raney nickel over a wide range

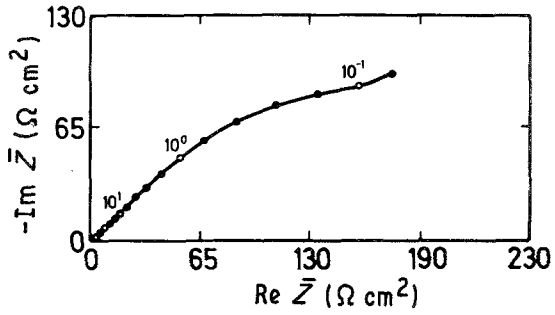

Fig. 6. Nyquist diagram of a rotating-disc Raney nickel electrode in 1 M NaOH solution at $E_H = -0.9$ V, rotation frequency, $f_{rot} = 30\,s^{-1}$ and $T = 303$ K.

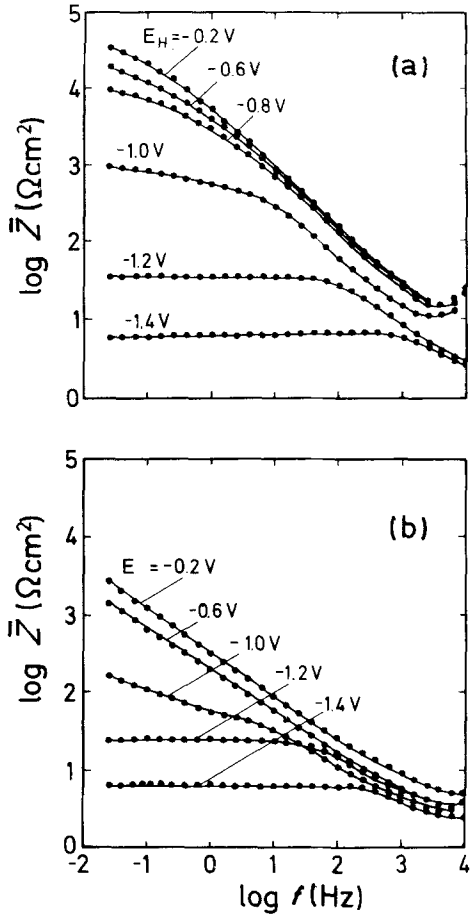

Fig. 7. Bode diagrams, log (|Z|) versus log (f), of a rotating-disc Raney nickel electrode in 1 M NaOH, T = 303 K, at different electrode potentials. (a) polarization from $E_H = -0.2$ V to $E_H = -1.4$ V and (b) polarization from $E_H = -1.4$ V to $E_H = -0.2$ V.

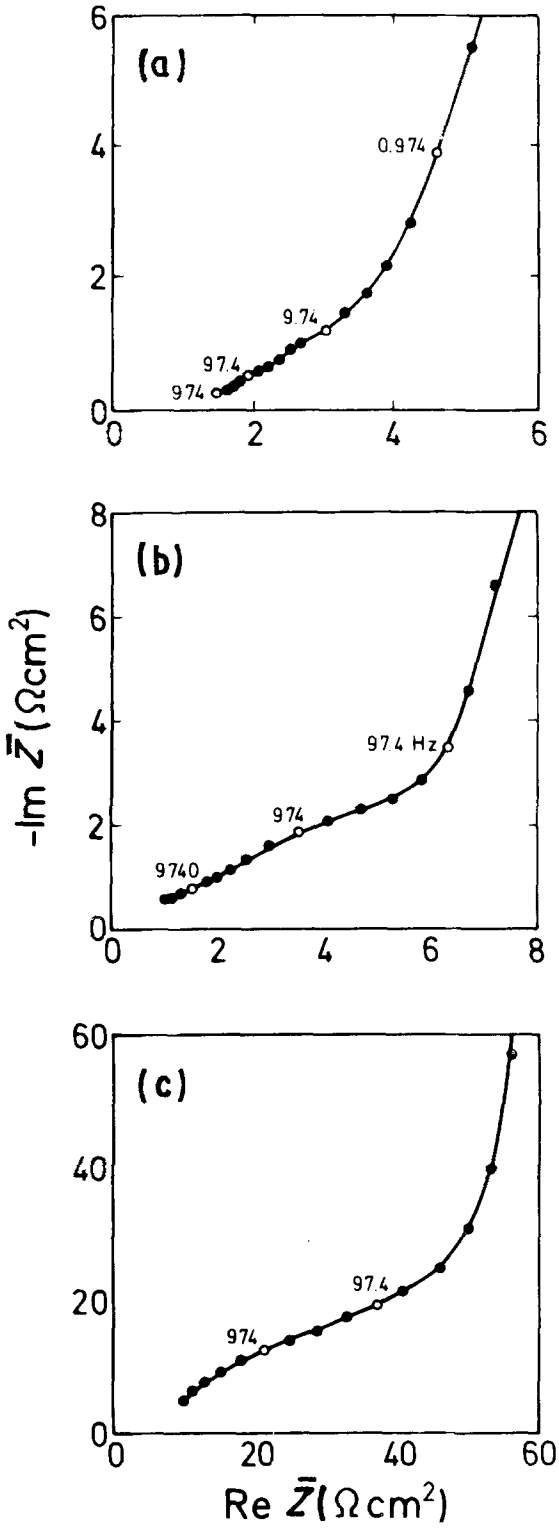

Fig. 8. Nyquist diagrams obtained under comparable conditions on (a) Raney nickel at $E_H = -0.3$ V, (b) graphite cloth (GC-10) and (c) graphite felt (GC-S3) at $E_H = -0.8$ V in 1 M NaOH solutions, T = 303 K.

of frequencies and polarization conditions. However, it should be noted that not all of the parameters in Equations 1–3 can be determined independently from non-linear curve-fitting of experimental impedance spectra. Rearrangement of Equation 3 leads to the following transfer function, $Z_p(s)$

$$Z_p(s) = R_{el} + R_{\Omega,p}\,(1/\lambda(s))^{1/2}\coth\,(\lambda(s))^{1/2} \quad (4)$$

where $R_{\Omega,p} = \rho l/n\pi r^2$ is the electrolyte resistance along the axis of n pores and $\lambda(s)$ is a function of three parameters A, B, and α

$$\lambda(s) = [1 + (sAB)^{\alpha}]/A \quad (5)$$

which are related to the system parameters R_t, C_{dl}, r, l, and ρ according to the following equations

$$A = aR_t;\quad B = C_{dl}/a;\quad \text{with } a = r/2\rho l^2 \quad (6)$$

Physically, the function $\lambda(s)$ corresponds to $R_{\Omega,pl}/Z_{w,pl}$, that is the ratio of the electrolyte resistance, $R_{\Omega,pl}$, and the wall impedance of a single pore $Z_{w,pl} = Z_0/2\pi rl$. Therefore, a fit of the experimental results using the transfer function defined by Equations 4 and 5 yields the five independent parameters R_{el}, $R_{\Omega,p}$, A, B, and α to be adjusted by a non-linear fit routine.

To demonstrate the quality of the fit, Fig. 9 shows two typical results in Nyquist and Bode representations, obtained in 6 M NaOH solution under cathodic and anodic polarization conditions. With the exception of a few points at high frequencies, there is relatively good agreement between experiment and fit results. Corresponding fits of impedance data obtained over the whole potential range of cathodic and anodic polarization and at different NaOH concentrations also gave satisfactory results. The sum of

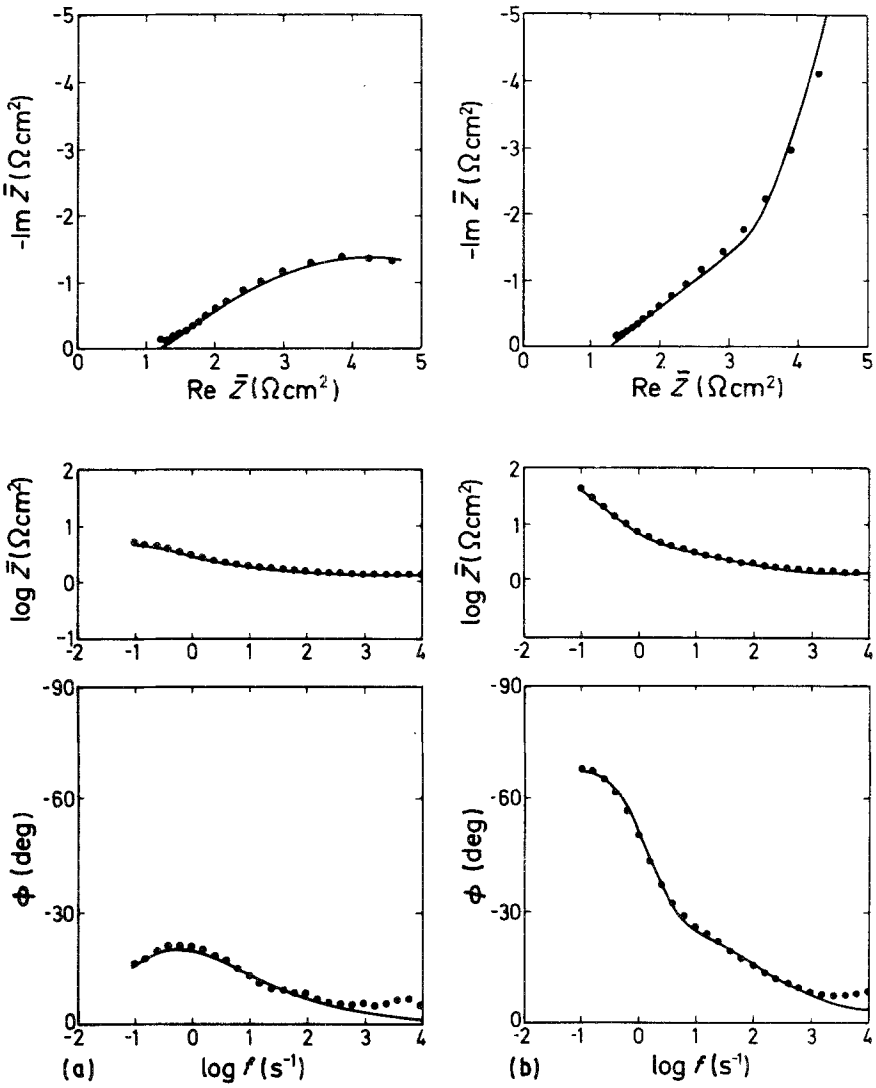

Fig. 9. Nyquist diagrams and Bode plots for Raney nickel at (a) $E_H = -0.8$ V and (b) $E_H = -0.2$ V in 6 M NaOH solution at $T = 303$ K; (●) experimental points and (——) fit results using the cylindrical pore model.

least squares, defined by $\Sigma_2 = \Sigma|\Delta Z/Z|^2$ with $\Delta Z = Z_{exp}(s) - Z_{theor}(s)$, was found to range between $0.02 \leqslant \Sigma_2 \leqslant 0.08$. The fit parameters A, B, α, and $R_{\Omega,p}$ for Raney nickel in 6 M NaOH are depicted in Fig. 10 as a function of the applied d.c. potential. Two complete experimental sets, corresponding to a polarization in cathodic and anodic directions were analysed and the results are identified by different symbols in Fig. 10.

The value of the empirical exponent α in Equation 2 varies so that $0.75 \leqslant \alpha \leqslant 0.86$, showing only a weak potential dependence. The parameters A, B and $R_{\Omega,p}$ in Fig. 10, however, undergo distinct changes at potentials where the transition from cathodic to anodic polarization takes place, compare with Fig. 2.

In particular, in the region of cathodic polarization, A increases exponentially with E_H by several orders of magnitude with a slope of $(\partial \log A/\partial E_H) \approx 8.33\,V^{-1}$. Since $A = aR_t$ and $R_t = 0.434\, b_-/i_{ss}$ for a charge-transfer-controlled reaction, where i_{ss} denotes the steady-state current density and $b_- = -(\partial E_H/\partial \log |i_{ss}|)$ is the Tafel slope of the cathodic reaction, it follows that $b_- = -(\partial E_H/\partial \log A) \approx -0.120$ V, corresponding to a charge-transfer coefficient of 0.5 and a charge-transfer valency of 1. This value is in accordance with the Tafel slope of the charge-transfer-controlled hydrogen-evolution reaction on nickel electrodes [23]. On the other hand, in the anodic polarization range a nearly constant value of A is found in Fig. 10. It is clear that the assumptions made in Equation 2 are not valid for a transport controlled process under anodic polarization. It should be noted that in this case the A values are about three orders of magnitude larger than those found under cathodic polarization conditions, indicating that $Z_0(s)$ in Equation 1 should be better approximated by a transport impedance of a high absolute value, due to limiting diffusion conditions of hydrogen molecules towards the wall of the pores, presumably through a thin film of oxidation products. In this case the overall impedance is mainly determined by the double-layer capacitance C_{dl}. This is also revealed in the impedance spectrum shown in Fig. 9 at $E_H = -0.2$ V, exhibiting a change of the capacitive phase-angle from about $-90°$ to $-45°$ due to 'squaring' of the interfacial impedance according to Equation 1 as the coth term becomes approximately 1 at higher frequencies. The same effect which is typical for systems with semi-infinite pores is also observed in most of the impedance results shown in Figs 3, 4, 5 and 8.

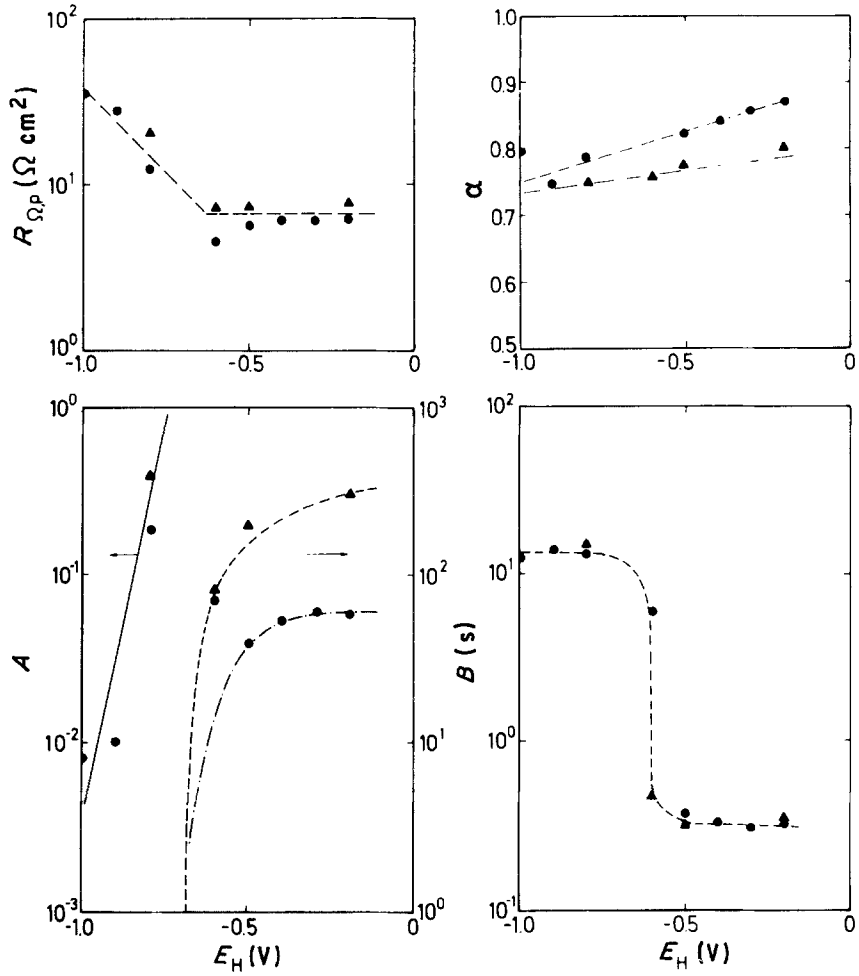

Fig. 10. Fit parameters $R_{\Omega,p}$, α, A, and B as a function of the electrode potential obtained from a fit of the impedance data of Raney nickel in 6 M NaOH at $T = 303$ K. (▲) correspond to cathodic polarization direction from $E_H = -0.2$ V to -1 V and (●) to anodic polarization direction from $E_H = -1$ V to -0.2 V.

The parameter B attains nearly constant values of $B \approx 14$ s and $B \approx 0.4$ s in the cathodic and the anodic region, respectively, whereas $R_{\Omega,p}$ is constant in the anodic part and increases only slightly under cathodic polarization.

As discussed above, the specific pore parameters r, l, and n cannot be determined independently from the fit parameters without additional information. From BET and SEM measurements the pore radius of Raney nickel is known to be in the order of $r \approx 10^{-6}$ cm [13, 18]. This allows estimation of the pore length l from the geometry factor $a = C_{dl}/B$ using typical values of $C_{dl} \approx 30\,\mu$F cm^{-2} and $\rho \approx 10\,\Omega$cm. The effective l values were found to be in the order of $l \approx 0.15$ cm in the cathodic and $l \approx 0.025$ cm in the anodic range. The difference may be explained by the fact that the anodic oxidation of H_2 in porous gas-diffusion electrodes mainly takes place at a three-phase boundary-zone. The slight increase of $R_{\Omega,p}$ under cathodic H_2 evolution conditions also indicates the formation of an H_2 gas phase in the pore system thus leading to a decreasing number of electrochemically active pores due to a partial blocking and displacement of the electrolyte. The overall number, n, of active pores can be evaluated directly from $R_{\Omega,p}$. A rough estimation of n using mean values of $R_{\Omega,p} \approx 10\,\Omega$cm^2 and $l \approx 0.08$ cm leads to a $n = 2 \times 10^{10}$ pores per cm^2 geometrical area of the catalyst electrode. A specific density of 10^7 pore mouths per cm^2 of true catalyst area is calculated assuming spherical grains with a mean radius of $r_g = 10^{-4}$ cm. This number is in good agreement with calculations of other authors [13, 18].

4. Conclusions

The dynamic studies of technical porous Raney nickel electrodes by means of electrochemical impedance spectroscopy (EIS) in the potential range of the hydrogen evolution and hydrogen oxidation reactions yield valuable information about the structural and electrocatalytic properties of the electrode material. A quantitative transfer-function analysis of the impedance spectra on the basis of a physical model and non-linear complex least-squares-fit procedure was applied to evaluate the kinetic and structural parameters of the system. The experimental results show that the dynamic response of porous electrodes can be described adequately over a wide range of pH and temperature of the solution for anodic and cathodic polarization conditions.

Acknowledgement

The authors acknowledge the financial support of this work by the Arbeitsgemeinschaft Industrieller For-

schungsvereinigungen (AIF). One of us (J. R. V.) is grateful to the Alexander von Humboldt Foundation for making this cooperation possible and (L. M. G.) thanks the Bundesministerium für Forschung und Technologie (BMFT) and the CONICET-Argentina for the fellowships granted.

References

[1] E. Justi and A. Winsel, 'Kalte Verbrennung', Franz Steiner Verlag, Wiesbaden (1962).
[2] W. Vielstich, 'Brennstoffelemente', Verlag Chemie, Weinheim (1965).
[3] F. von Strum, 'Elektrochemische Stromerzeugung', Verlag Chemie, Weinheim (1969).
[4] A. Winsel, *Z. Electrochemie* **66** (1962) 287.
[5] L. G. Austin, *Trans. Faraday Soc.* **60** (1964) 1319.
[6] S. K. Rangarajan, *J. Electroanal. Chem.* **22** (1969) 89.
[7] K. Mund, *Siemens Forsch. u. Entwickl. Ber.* **4** (1975) 1.
[8] K. Mund, G. Richter, E. Weidlich, F. von Sturm and E. David, *Bioelectrochemistry and Biogenetics* **3** (1979) 272.
[9] D. Wabner, R. Holze and P. Schmittinger, *Z. Naturforschung* **39b** (1984) 157.
[10] R. Holze and A. M. Castro Luna, *J. Appl. Electrochem.* **18** (1988) 679.
[11] R. de Levie, in 'Advances in Electrochemistry and Electrochemical Engineering', Vol. 6 (edited by P. Delahay and C. W. Tobias) John Wiley & Sons, New York (1967) p. 329.
[12] M. Keddam, C. Rakotomavo and H. Takenouti, *J. Appl. Electrochem.* **14** (1984) 437.
[13] J. -P. Candy, P. Fouilloux, M. Keddam and H. Takenouti, *Electrochim. Acta.* **27** (1982) 1585.
[14] C. Cachet and R. Wiart, *ibid.* **29** (1984) 145.
[15] J. -P. Candy, P. Fouilloux, C. Gabrielli, M. Keddam and H. Takenouti, *C. R. Acad. Sc. Paris* **285** (1977) 463.
[16] J. -P. Candy, P. Fouilloux, M. Keddam and H. Takenouti, *Electrochim. Acta* **26** (1981) 1029.
[17] K. Mund, G. Richter and F. von Sturm, Proceedings of the Workshop on Electrocatalysis of Fuel Cell Reactions, Vol. 2 (edited by W. E. O'Grady, S. Srinivasan and R. F. Dudley) The Electrochemical Society, Princeton, New Jersey (1979) p. 47.
[18] K. Mund, G. Richter and F. von Sturm, *J. Electrochem. Soc.* **124** (1977) 1.
[19] N. A. Hampson and A. J. S. McNeil, in Specialist Periodical Report on Electrochemistry, Vol. 8 (edited by D. Pletcher) The Royal Society of Chemistry, London (1983) p. 1.
[20] K. Mund, M. Edeling and G. Richter, in Proceedings of the Symposium on Porous Electrodes: Theory and Practice, Vol. 8 (edited by H. C. Maru, T. Katan and M. G. Klein) The Electrochemical Society, Pennington, New Jersey (1984) p. 336.
[21] C. Cachet and R. Wiart, *J. Electroanal. Chem.* **195** (1985) 21.
[22] A. Winsel, *Dechema Monographs* **98** (1985) 181.
[23] A. J. Appleby, H. Kita, M. Chemla and G. Bronoel, in 'Encyclopedia of Electrochemistry of the Elements', Vol. IX-A, (edited by A. J. Bard) Marcel Dekker, New York (1982) 383.